scientific reports

Check for updates

OPEN

Dynamical dissipative and radiative flow of comparative an irreversibility analysis of micropolar and hybrid nanofluid over a Joule heating inclined channel

S. Suresh Kumar Raju

This report scrutinized the influence of radiation and Ohmic heating on the dissipative flow of micropolar and hybrid nanofluid within an inclined length 2*h* channel under convective boundary conditions. Primary flow equations are renewed as the system of NODEs with the assistance of proper similarity conversions. In two circumstances, hybrid fluid flow and micropolar fluid flow, a blend of shooting and Runge–Kutta 4th order strategy, is used to achieve the desired results. The critical consequences of the current study are Larger pressure gradient minimizes the fluid velocity, and a more significant inertia parameter minimizes the rotation profile in the case of Newtonian fluid flow but facilitates the same in the case of hybrid nanofluid flow. It is perceived that the escalation in Brinkmann number causes the amelioration in the fluid temperature, and the radiation parameter mitigates the same. Furthermore, it is discovered that the Grashoff number enhances the Bejan number at the centre of the channel but lessens the same at other areas. Finally, validation is executed to compare the current outcomes with the former results and perceive a good agreement.

Hydrous or unsteady globes might also be electrically conductive and capable of withstanding core fluxes commencing electromagnetic stimulation. Instances of this occurrence are occasionally named induction boiler or Joule heating. These constituents of ohmic heating are offered in various manufacturing, industrial and cosmological sceneries. By viewing this, Makinde and Gbolagade[1] investigated entropy generation in a laminar viscous fluid flow via an inclined passage. They discovered that fluid friction's irreversibility dominated heat transfer's irreversibility on the channel centerline. Guimaraes and Menon[2] conducted a heat transmission investigation of mixed convective fluid within an inclined channel (rectangular) with the help of the finite element technique. Dar and Elangovan[3] inspected the impact of a magnetic field on the peristaltic flow through an inclined channel (asymmetric) and acknowledged that the magnetic field lessens the fluid velocity. Shahri and Sarhaddi[4] emphasized that the main reason for entropy generation is the heat conduction of nanofluid (water–Cu) in their examination of MHD fluid flow within an inclined channel. By assuming a low Reynolds number and considering an inclined channel, Javed et al.[5] scrutinized the peristaltic flow with the Hartmann number. They concluded that the Hartmann number escalates the trapped bolus size. Hayat et al.[6] analyzed the peristaltic transport of the pseudoplastic fluid flow in the same parameter with heat source and Joule heating. Reynolds number ameliorates the fluid temperature is one of the findings of this study. Tlau and Ontela[7] considered convective conditions and elucidated the mixed convective flow of $H_2O + Cu$ a tended channel occupied with a permeable medium. They observed the enhancement in the fluid velocity with a greater inclination angle. With the assumption of the same geometry, Adesanya et al.[8] and Singh et al.[9] proposed a model for different fluid flows to discuss the irreversibility analysis. They discovered that there is a reduction in the entropy generation rate with a couple of stress parameters. Sabu et al.[10] used a correlation coefficient to examine the features of engineering parameters in an unsteady MHD nanofluid flow with the heat source. They detected that the Soret number is negatively affiliated

Department of Mathematics and Statistics, College of Science, King Faisal University, Al-Ahsa 31982, Saudi Arabia. email: ssurapuraju@kfu.edu.sa

with the Sherwood number. Several researchers[11–14] recently examined different fluid flows (including hybrid nanofluid) via similar geometry and highlighted that inclined geometry control the flow and heat transfer process.

Improvement in the transfer of heat across fluid movement has made authorities in thermal manufacturing encirclement the efficiency of a combination of solid nanoparticles called a Hybrid nanofluid. The previously revealed improvement is based on the nature of the base fluid and nanoparticles. Solid particle concentration and thermal properties on the proportion of mass to density and viscidness are precisely the physical possessions. Nevertheless, thermal conductivity and specific heat capacity at different intensities of concentration of nano-solid particles, nanoparticles' size, and temperature are some of the thermal possessions. Considering this, Gholinia et al.[15] illustrated the MHD flow of a nanofluid (Ethylene glycol + Silver + Copper) by a circular cylinder with injection/suction. They concluded that the silver nanoparticles are better than copper when a higher temperature is required. Nadeem et al.[16] numerically investigated a nanofluid (Water + SWCNT) flow by a curled sheet with a magnetic field. They observed that the volume fraction of nanoparticles ameliorates the fluid temperature. Sowmya et al.[17] assumed longitudinal fin as geometry and examined the convective flow of a nanofluid (alloys of titanium and aluminium) with radiation. Dogonchi et al.[18] inspected the radiative flow of $Cu + H_2O$ fluid with a heat source and two reactions (heterogeneous–homogeneous) by a flat plate. They found a positive association between the Nusselt number and the magnetic field parameter. Newly, Anuar et al.[19] and Waqas et al.[20] assumed distinct geometries and scrutinized different water-based nanofluid flows under various conditions. Jamshed and Aziz[21] did an irreversibility analysis on the Casson HNF ($TiO_2 - CuO/EG$) flow by an elongating surface with the CCHF model. They found that the Brinkman number escalates the entropy generation. Salman et al.[22] considered FFS and BFS and reviewed various hybrid nanofluid flows. They opined that HNFs are the best alternates compared to mono NFs when better thermal features are required. Abbas et al.[23] assumed a thin needle and inspected the forced convective flow of an HNF (Water + SWCNT + MWCNT) with variable thermal conductivity. Anuar et al.[24] and Waini et al.[25] delivered a stability study for the radiative HNF ($Cu - Al_2O_3/Water$) flow by a revolving shrinking/elongating sheet. Based on that, they categorized the solutions as stable and unstable. Recently, various researchers[26–37] considered different geometries as well as the combination of solid nanoparticles and generated intermediate kinds of conductivity properties. This helps us to highlight the intermediatory processes.

Once the careful insight of the earlier stated inscription, we propose to discourse the importance of the radiation and Ohmic heating on the dissipative flow of micropolar and combination of solid nanoparticles (Propylene glycol – Water mixture + Paraffin Wax + Sand) by a tended channel. Results are offered in two examples, i.e., micropolar fluid and HNF. Further, irreversibility analysis is performed for the fluid flow against various pertinent parameters. The outcome of such investigation could be useful to identify the performances of nanoparticles and their effectiveness in microchannels filled with low conductivity properties. The following investigation was modelled to provide the answers to the following related research queries.

1. When non-linear energy and mass flux due to concentration and thermal gradient are negligible, what is the importance of the growing radius of solid nanoparticles on the entropy generation and Bejan numbers?
2. At different intensities of energy and momentum fluxes due to gradients in momentum and thermal, respectively, how do PEG-based Magnesium oxide (MgO) and Zirconium oxide (ZrO_2) nanoparticles influence the transport phenomena of an inclined channel?
3. When irreversibility takes place, what variations are availed for micro-polar and hybrid nanofluid?

Mathematical formulation

In this model, we have considered a non-transient steady laminar incompressible radiative hybrid and micropolar nano fluid flow in a microchannel of width h. Magnesium oxide (MgO) and Zirconium oxide (ZrO_2) nanoparticles are considered with a base fluid polyethene glycol (PEG). Values of the thermo-physical attributes are presented in Table 1.

The channel, which has an inclination angle α, is formed by two plates (upper and lower), separated by a distance $2h$ and positioned at $y = h$ and $y = -h$ correspondingly. The x axis is located in the centre of the channel, which indicates the direction of the flow. Let the bottom plate of the microchannel exchange the hot fluid temperature T_2 via convection, whereas the top plate is in contact temperature with the ambient fluid temperature T_1. Magnetic field (MHD) of potential strength B_0 is imposed in the y direction, to record its influence on flow and heat transformation. The above stated assumptions are depicted in Fig. 1.

Under the above-mentioned assumptions, the flow governing equations following (Srinivasacharya and Bindu[38], Xiangcheng and Shiyuan Li[39] and Roja et al.[40]), are

$$\upsilon = \upsilon_0 \tag{1}$$

$$\mu_{hnf}(1+\kappa)\frac{\partial^2 u}{\partial y^2} - \rho_{hnf}\upsilon_0\frac{\partial u}{\partial y} + \kappa\frac{\partial N}{\partial y} + (\rho\beta)_{hnf}g(T - T_1)\sin(\alpha) - \sigma B_0^2 u - \frac{\partial p}{\partial x} = 0 \tag{2}$$

$$\gamma\frac{\partial^2 N}{\partial y^2} - \rho_{hnf}j\upsilon_0\frac{\partial N}{\partial y} - 2\kappa N - \kappa\frac{\partial u}{\partial y} = 0 \tag{3}$$

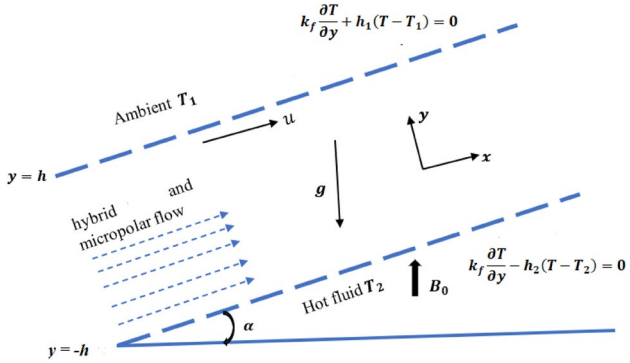

Figure 1. Representation of the flow.

S.no		Polyethylene glycol–water mixture (f)	$ZrO_2\,(s_1)$	$MgO\,(s_2)$
1	$\rho\,(\mathrm{Kg/m^3})$	1110	5680	3560
2	$k\,(\mathrm{Wm^{-1}K^{-1}})$	0.3712	1.7	45
3	$C_p\,(\mathrm{JKg^{-1}K^{-1}})$	3354	502	955

Table 1. Numerical values of thermophysical attributes convoluted in HNF (Hossainy and Eid[41]).

$$\left(k_{hnf}+\frac{16\sigma*T_1^3}{3k*}\right)\frac{\partial^2 T}{\partial y^2}-(\rho C_p)_{hnf}\upsilon_0\frac{\partial T}{\partial y}+\begin{pmatrix}\mu_{hnf}\\+\kappa\end{pmatrix}\left(\frac{\partial u}{\partial y}\right)^2+2\kappa\left(N^2+N\frac{\partial u}{\partial y}\right)+\begin{pmatrix}Q_T^*(T-T_1)\\+\sigma B_0^2 u\end{pmatrix}+\gamma\left(\frac{\partial N}{\partial y}\right)^2=0 \tag{4}$$

with the conditions (Srinivasacharya and Bindu[38])

$$at\ y=-h:\ u=0,\ N=-n\frac{\partial u}{\partial y},\ k_f\frac{\partial T}{\partial y}\ -h_2(T-T_2)=0 \tag{5}$$

$at\ y=h:\ u=0,\ N=0,\ k_f\frac{\partial T}{\partial y}+h_1(T-T_1)=0$and

$\rho_{hnf}=(1-\phi_2)\left[(1-\phi_1)\rho_f+\phi_1\rho_{s_1}\right]+\phi_2\rho_{s_2}$	$\frac{\sigma_{nf}}{\sigma_f}=1/\left(\frac{\sigma_{s_1}+2\sigma_f+\phi_1(\sigma_f-\sigma_{s_1})}{\sigma_{s_1}+2\sigma_f-2\phi_1(\sigma_f-\sigma_{s_1})}\right)$
$\mu_{hnf}=\frac{\mu_f}{(1-\phi_1)^{2.5}(1-\phi_2)^{2.5}}$	$k_{hnf}=\frac{k_{s_2}+2k_{nf}-2\phi_2(k_{nf}-k_{s_2})}{k_{s_2}+2k_{nf}+\phi_2(k_{nf}-k_{s_2})}\times k_{nf}$
$\sigma_{hnf}=\frac{\sigma_{s_2}+2\sigma_{nf}-2\phi_2(\sigma_{nf}-\sigma_{s_2})}{\sigma_{s_2}+2\sigma_{nf}+\phi_2(\sigma_{nf}-\sigma_{s_2})}\times\sigma_{nf}$	$k_{nf}=\frac{k_{s_1}+2k_f-2\phi_1(k_f-k_{s_1})}{k_{s_1}+2k_f+\phi_1(k_f-k_{s_1})}\times k_f$
$(\rho C_p)_{hnf}=(1-\phi_2)\left[(1-\phi_1)(\rho C_p)_f+\phi_1(\rho C_p)_{s_1}\right]+\phi_2(\rho C_p)_{s_2}$	

where N-micro rotation, $K=\frac{\kappa}{\mu_f}$—micro polar parameter, κ—vortex viscosity,ρ the density, μ the dynamic viscosity, j the gyration parameter, g is the gravitation, β the thermal expansion coefficient, q_r the radiative heat flux, σ the electrical conductivity, γ the spin gradient viscosity and $\gamma=\left(\mu_{nf}+\frac{\kappa}{2}\right)j=\mu_f\left(\frac{\mu_{nf}}{\mu_f}+\frac{K}{2}\right)j$, and h_1, h_2 —the convective heat transfer coefficient for the individual plate. n Constant and $0\le n\le 1$ ($n=0$ represents strong concentration, $n=0.5$ anti-symmetric part of the stress tensor which represents weak concentration, $n=1$ is considered while modelling flow problem related to turbulent boundary layer). ϕ_1 and ϕ_2 the volume fraction of MgO and ZrO_2 nanoparticles, subscripts hnf specifies hybrid nanofluid (two nanomaterials + one base fluid), nf specifies nano liquid (one nanomaterial + base liquid), s_1 and s_2 specifies solid particles (1-MgO, 2-ZrO_2) and f requires base liquid (-polyethylene glycol (PEG)), $k*$ mean absorption coefficient and $\sigma*$ Stefan-Boltzmann constant.

Employing the subsequent non-dimensional variables (Roja et al.[40])

$$\zeta=\frac{y}{h},\ \ u=U_0 f(\zeta),N=\frac{U_0}{h}g(\zeta),\ \ T=T_1+(T_2-T_1)\theta(\zeta) \tag{6}$$

in Eqs. (2)–(5), following the non-linear system of ODEs and their associated boundary conditions are obtained.

$$(1+K)\frac{d^2f}{d\zeta^2} = A_2\left[RA_1\frac{df}{d\zeta} - K\frac{dg}{d\zeta} - \frac{Gr}{\mathrm{Re}}A_3\theta\sin\alpha + Mf + A\right] \tag{7}$$

$$\frac{d^2g}{d\zeta^2} = \left(\frac{2A_2}{2+K}\right)\left(\frac{1}{a_j}\right)\left[A_1Ra_j\frac{dg}{d\zeta} + 2Kg - K\frac{df}{d\zeta}\right] \tag{8}$$

$$\frac{d^2\theta}{d\zeta^2} = \left(\frac{1}{A_4A_{41} + \frac{4}{3}Ra}\right)\left[A_5\,\mathrm{Pr}\,\frac{d\theta}{d\zeta} - Br\left(\begin{array}{l}\left(\frac{1}{A_2}+K\right)\left(\frac{df}{d\zeta}\right)^2 + 2K\left(\left(g(\zeta)\right)^2 + g(\zeta)\frac{df}{d\zeta}\right)\\ +M\left(f(\zeta)\right)^2 + \left(\frac{2+K}{2A_2}\right)a_j\left(\frac{dg}{d\zeta}\right)^2\end{array}\right) + Q_t\theta\right] \tag{9}$$

$$at\ \zeta = -1:\ f = 0,\ g = -n\frac{d^2f}{d\zeta^2},\ \frac{d\theta}{d\zeta} - Bi_2(\theta - 1) = 0 \tag{10}$$

$at\ \zeta = 1:\quad f = 0,\ g = 0,\quad \frac{d\theta}{d\zeta} + Bi_1(\theta) = 0.$

In the above equations,

$A_1 = (1-\phi_2)\left[(1-\phi_1) + \phi_1\frac{\rho_{s_1}}{\rho_f}\right] + \phi_2\frac{\rho_{s_2}}{\rho_f}$	$A_4 = \frac{k_{s_2}+2A_{41}k_f - 2\phi_2(A_{41}k_f - k_{s_2})}{k_{s_2}+2A_{41}k_f + \phi_2(A_{41}k_f - k_{s_2})}$
$A_2 = (1-\phi_1)^{2.5}(1-\phi_2)^{2.5}$	$A_{41} = 1/\left(\frac{k_{s_1}+2k_f+\phi_1(k_f-k_{s_1})}{k_{s_1}+2k_f-2\phi_1(k_f-k_{s_1})}\right)$
$A_3 = (1-\phi_2)\left[(1-\phi_1) + \phi_1\frac{(\rho\beta)_{s_1}}{(\rho\beta)_f}\right] + \phi_2\frac{(\rho\beta)_{s_2}}{(\rho\beta)_f}$	$A_5 = (1-\phi_2)\left[(1-\phi_1) + \phi_1\frac{(\rho C_p)_{s_1}}{(\rho C_p)_f}\right] + \phi_2\frac{(\rho C_p)_{s_2}}{(\rho C_p)_f}$

$R = \frac{\rho_f v_0 h}{\mu_f}$ the suction/injection, $\mathrm{Pr} = \frac{\mu_f(C_p)_f}{k_f}$ the Prandtl number, $Gr = \frac{\rho_f^2 g\beta_f(T_2-T_1)h^3}{\mu_f^2}$ the Grashof number, $Br = \frac{\mu_f U_0^2}{k_f(T_2-T_1)}$ the Brinkman number, $A = \frac{h^2}{\mu_f U_0}\frac{dp}{dx}$ the constant pressure gradient, $Q_t = \frac{Q_T^* a^2}{k_f}$ the Fourier heat source or sink, $M = \frac{\sigma B_0^2 h^2}{\mu_f}$ the magnetic number, $\mathrm{Re} = \frac{\rho_f U_0 h}{\mu_f}$ the Reynolds number, $Bi_i = -\frac{hh_i}{k_f}$ *for* $i = 1, 2$ the Biot number, $a_j = \frac{j}{h^2}$ the micro-inertia parameter, $Ra = \frac{4\sigma * T_1^3}{k_f k*}$ the radiation parameter.

Entropy optimization. The volumetric rate of entropy optimization is given (Srinivasacharya and Bindu[38], Roja et al.[40]) as

$$S_G = \frac{k_f}{T_1^2}\left[\frac{k_{hnf}}{k_f} + Ra\right]\left(\frac{\partial^2 T}{\partial y^2}\right) + \frac{\mu_{hnf}}{T_1}\left(\begin{array}{l}1\\ +\kappa\end{array}\right)\left(\frac{\partial u}{\partial y}\right)^2 + \frac{2K\mu_f}{T_1}\left[\begin{array}{l}N^2\\ +N\frac{du}{dy}\end{array}\right] + \frac{\gamma}{T_1}\left(\frac{\partial u}{\partial y}\right)^2 + Q_t(T - T_1) + \frac{\sigma B_0^2 u^2}{T_1}. \tag{11}$$

With the assistance of (6), Eq. (11) can be revised as

$$Ns = \left[\frac{k_{hnf}}{k_f} + Ra\right]\left(\frac{d^2\theta}{d\zeta^2}\right) + Q_t\theta + \frac{Br}{T_p}\left(\begin{array}{l}\frac{1}{A_2}(1+K)\left(\frac{df}{d\zeta}\right)^2 + 2K\left(\left(g(\zeta)\right)^2 + g(\zeta)\frac{df}{d\zeta}\right)\\ +M\left(f(\zeta)\right)^2 + \left(\frac{2+K}{2A_2}\right)a_j\left(\frac{dg}{d\zeta}\right)^2\end{array}\right)$$

where $N_s = \frac{h^2T_1^2}{k_f(\Delta T)^2}S_G$ is the dimensionless entropy and $T_p = \frac{\Delta T}{T_1}$.

The Bejan number is given by,

$$Be = \frac{\text{Irreversibility as a outcome of mass and heat transmission}}{\text{Total irreversibility}}.$$

That is,

$$Be = \frac{\left[\frac{k_{hnf}}{k_f}\right]\left(\frac{d^2\theta}{d\zeta^2}\right)}{\left[\frac{k_{hnf}}{k_f}\right]\left(\frac{d^2\theta}{d\zeta^2}\right) + \frac{Br}{T_p}\left(\begin{array}{l}\frac{1}{A_2}(1+K)\left(\frac{df}{d\zeta}\right)^2 + 2K\left(\left(g(\zeta)\right)^2 + g(\zeta)\frac{df}{d\zeta}\right)\\ +M\left(f(\zeta)\right)^2 + \left(\frac{2+K}{2A_2}\right)a_j\left(\frac{dg}{d\zeta}\right)^2\end{array}\right)}.$$

Results and discussion

To solve the transmuted equations, a blend of shooting and Runge–Kutta 4th order strategies is used. In this study, results are provided in two cases, hybrid nanofluid and micropolar fluid.

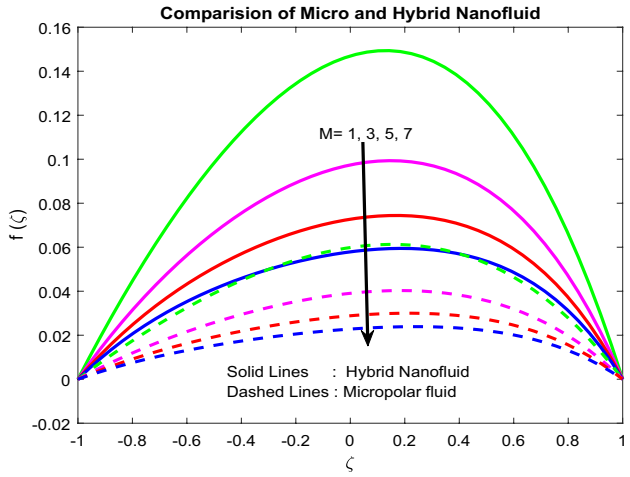

Figure 2. Impact of Bi_2.

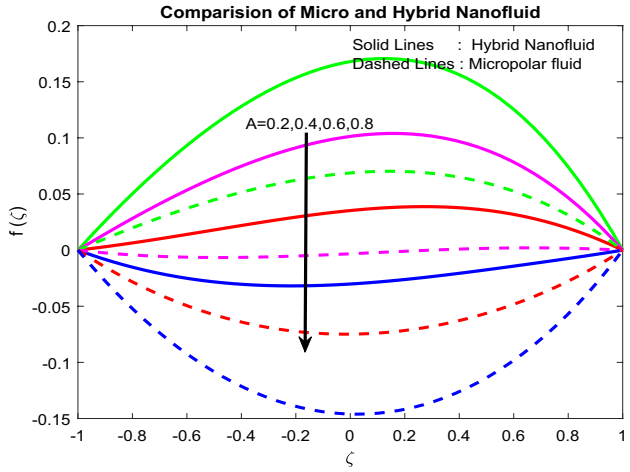

Figure 3. Impact of A.

Velocity and microrotation profiles. The fluid motion is pretentious by a magnetic field. The constituent part of fluid erection, a chain, turns in the direction of the applied attractive field. For the period of this time, the solid particles collide with each other, forming a barrier to the fluid flow. As an outcome, fluid momentum minimizes owing to the upsurge in the viscosity of the liquid (Fig. 2). From Fig. 3, and it is detected that the more significant pressure gradient minimizes the fluid velocity. Physically as expected, the pressure gradient generates higher forces opposing the flow direction, and this causes depreciation in the velocity field. Generally, with the rise in Grashoff number, viscous forces reduce. As a consequence, velocity upsurges (Fig. 4). Figure 5 explicates the fact that the larger inertia parameter minimizes the rotation profile in the case of Newtonian fluid flow and ameliorates the same in the case of hybrid nanofluid flow. Note that the increment in the inertia parameter minimizes the rotation of the particles.

Temperature profiles. Figure 6 revealed the fact that the Biot number near the lower channel minimizes the fluid temperature. Typically, with the rise in the Biot number, there is an escalation in the temperature gradient in a positive manner near the lower channel. So, temperature decreases. The higher the value of Br, the slower the conduction of heat delivered by viscous dissipation and, subsequently, the bigger the temperature rise (Fig. 7). Figure 8 uncovered that the heat source enriches the fluid temperature. Usually, a higher heat source affects the production of extra hotness inside the liquid and, in order, assists to enhances the thermal boundary. Magnetic field and radiation parameters mitigate the fluid temperature (Figs. 9, 10). Usually, as raising of values,

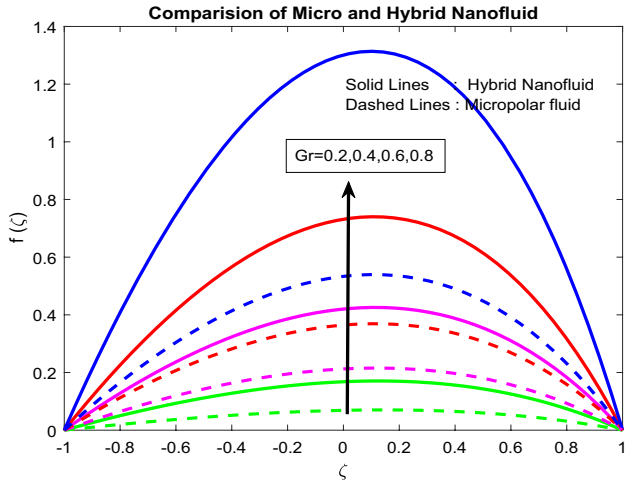

Figure 4. Impact of *Gr*.

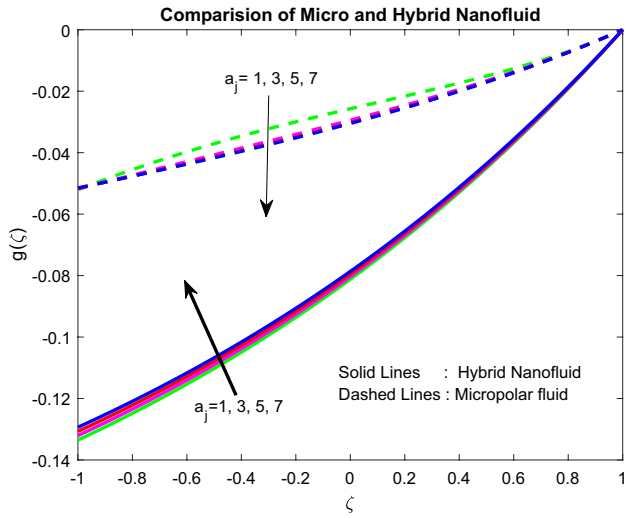

Figure 5. Impact of a_j.

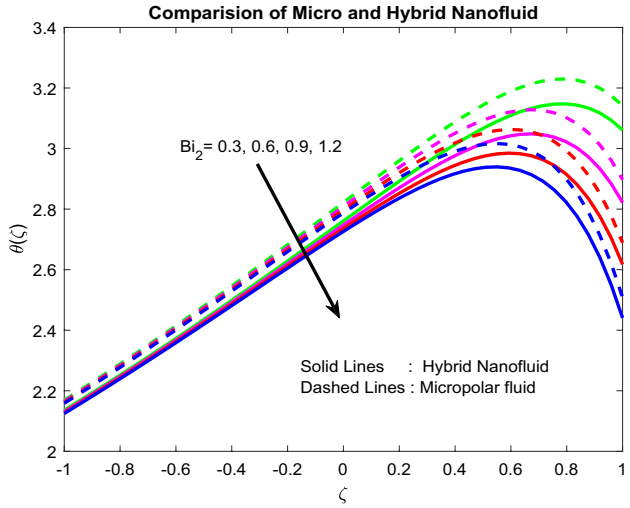

Figure 6. Impact of Bi_2.

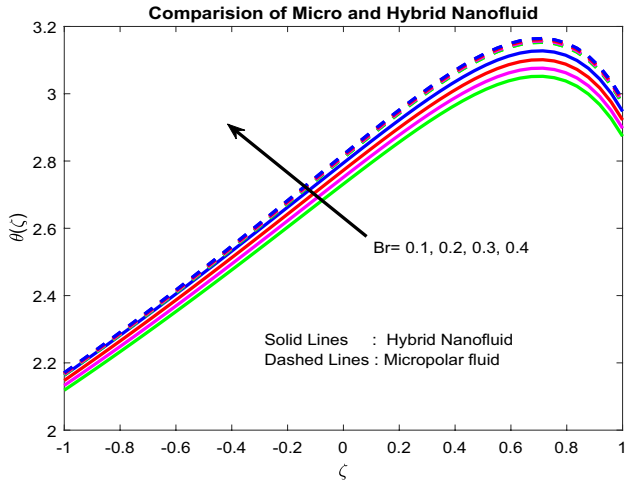

Figure 7. Impact of *Br*.

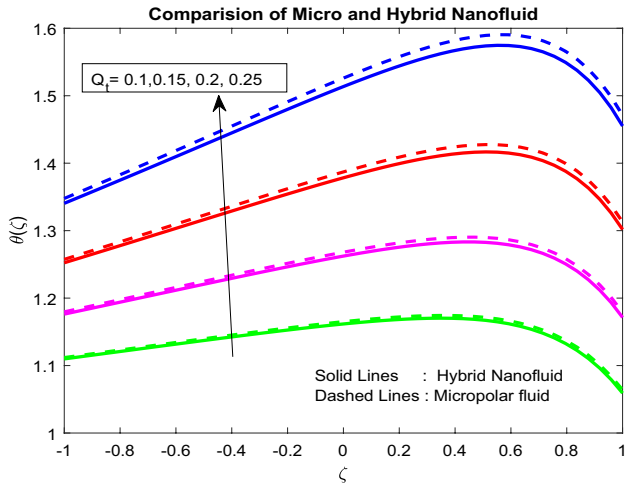

Figure 8. Impact of Q_t.

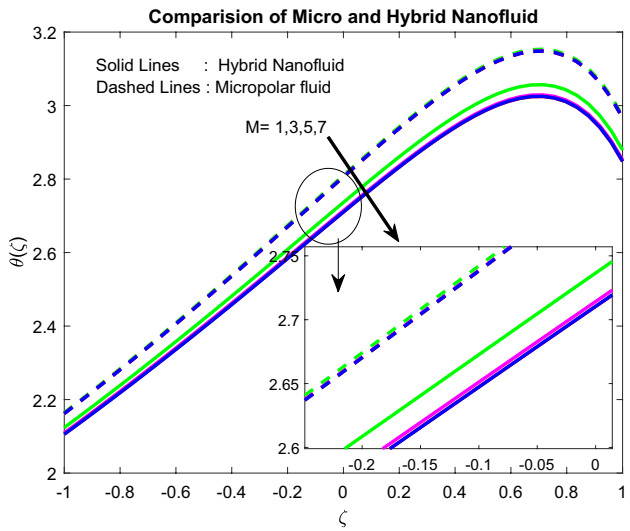

Figure 9. Impact of *M*.

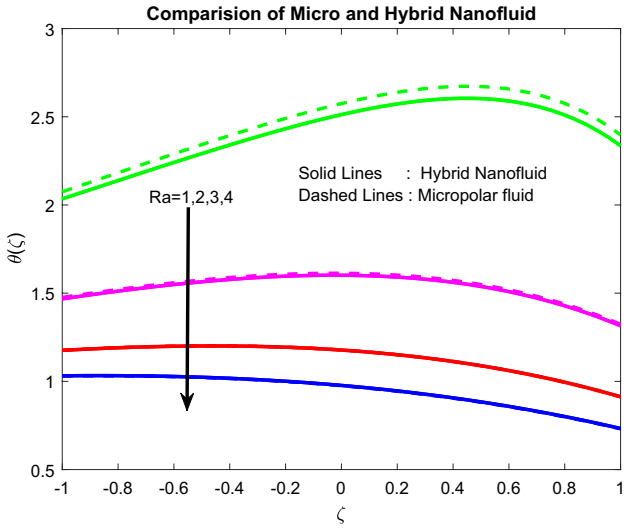

Figure 10. Impact of *Ra*.

these parameters generate high heat energy and particle interaction. Whereas the inclined nature of the channel sometimes makes to opposes the general physical behaviour, due to this reason, it was reduced.

Entropy generation and bejan number profiles. Figures 11, 12, 13, 14, 15 exhibit the impact of distinct parameters on the entropy generation profile. It is detected that Bi_2,Br,a_j, Ra and Gr are escalating the entropy generation. Note that viscous forces exert friction in fluid flow, which is the primary cause of entropy generation. Bejan number is the proportion of irreversibility because of heat transfer to entire irreversibility because of fluid friction and heat transfer and fluid friction. As raising Bi_2 improves the convective nature in the help, this helps to encourage the entropy generation, which is displayed in Fig. 11. As micro-inertia impact on entropy generation is shown in Fig. 13 and it is found that improved with a_j. Since micro inertia is proportional to the entropy generation. A quite similar performance was observed as the raising of Brickman number in Fig. 12. The Fig. 14 displays the thermal radiation on entropy generation. Thermal radiation creates a higher energy to move heat molecules faster, and due to this reason, observed enhancement. As the Grashof number establishes higher pressure, this help to improve interfacial particle transfer, which causes to grow the entropy generation, which is displayed in Fig. 15.

Figures 16, 17, 18 explicated the impact of Gr, M and a_j on Bejan number. It was discovered that Gr it ameliorates the Be Bejan number at the midpoint of the channel and minimizes the same at other areas (Fig. 16). This may be owing to the domination of heat transmission irreversibility associated to total irreversibility at the

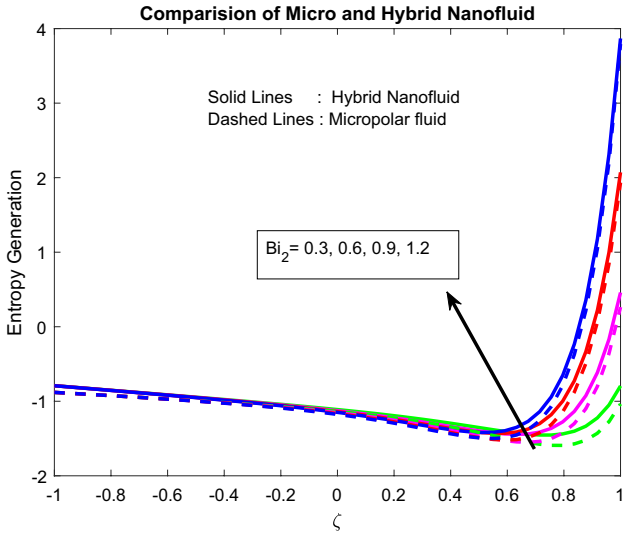

Figure 11. Impact of Bi_2.

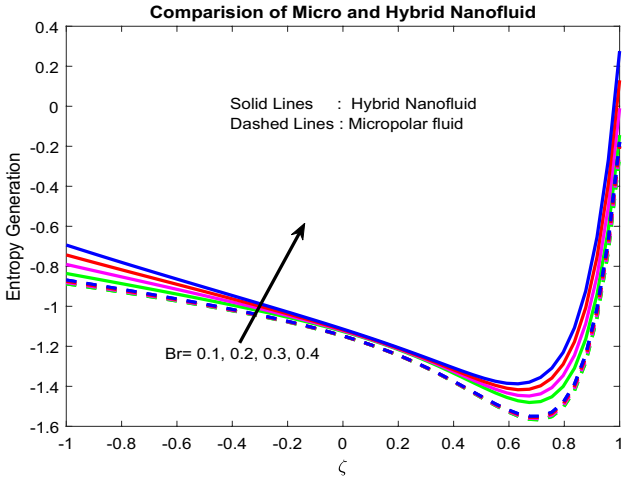

Figure 12. Impact of *Br*.

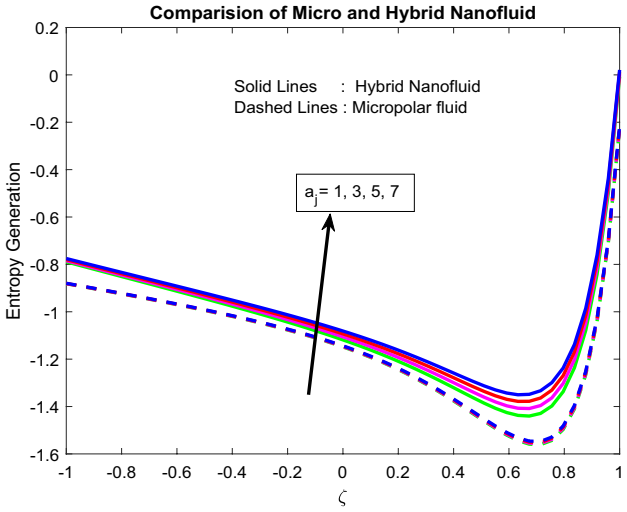

Figure 13. Impact of a_j.

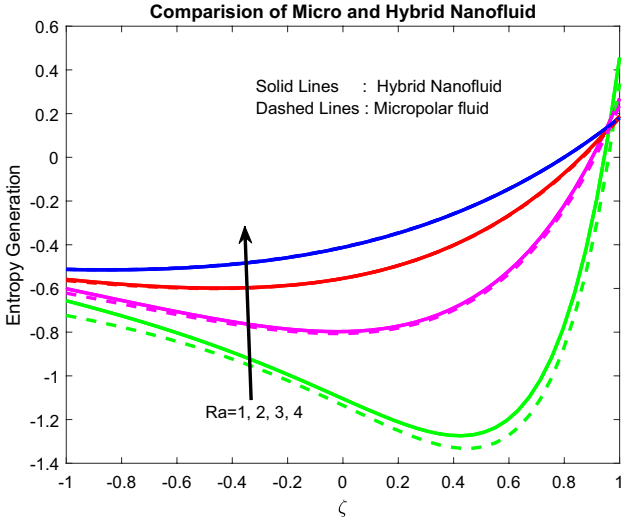

Figure 14. Impact of *Ra*.

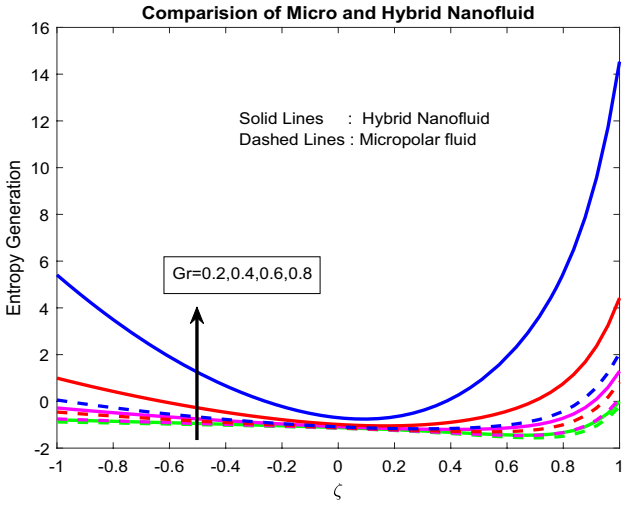

Figure 15. Impact of *Gr*.

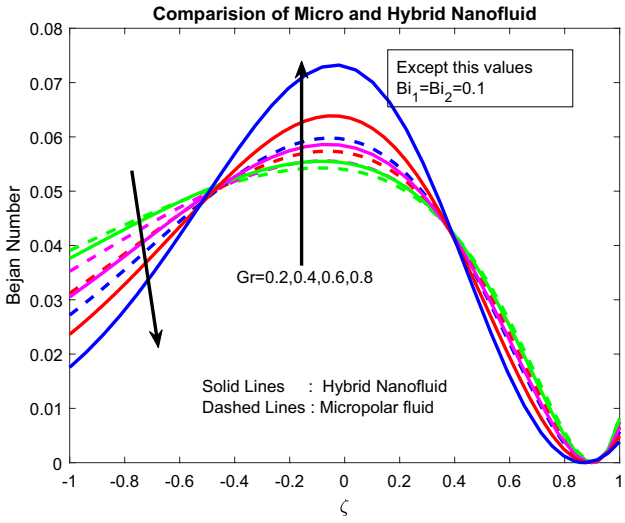

Figure 16. Impact of *Gr*.

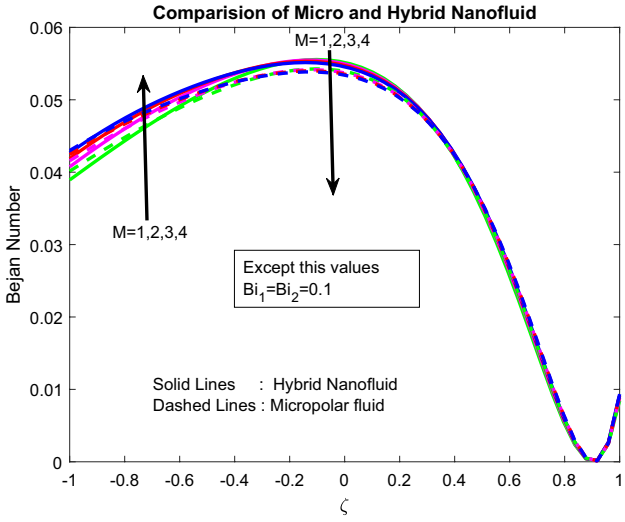

Figure 17. Impact of *M*.

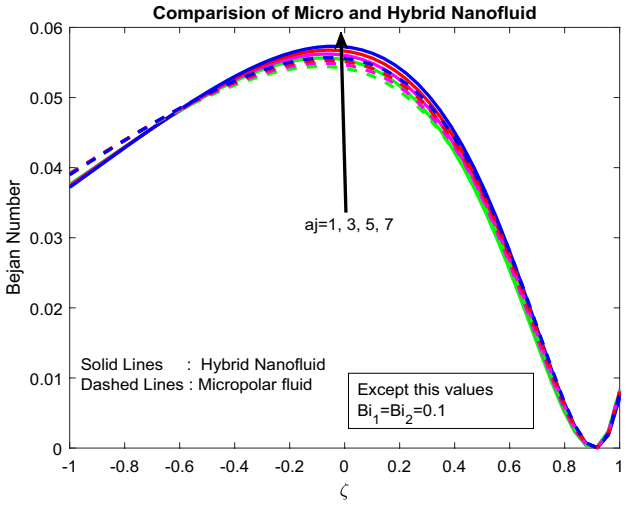

Figure 18. Impact of a_j.

centre of the channel. Parameters M and a_j are showing mixed behaviour on Bejan number (Figs. 17, 18). As the well-known fact is, the Bejan number is inversely proportional to the Parameters M and a_j. But interestingly, the inclined, irreversibility, and convective nature of the flow makes the flow performance in chaotic nature.

Validation. The current solutions are validated with the existing solution under limited case ($\phi_1 = \phi_2 = Gr = M = Q_t = n = Ra = R = 0, A = \mathrm{Re} = 1, aj = 0$) with the Makinde and Eegunjobi[42] is shown in Table 2 and found the excellent agreement with those solutions, this help to move further.

Conclusion

Hydrous or unsteady globes might also be electrically conductive and capable of withstanding core fluxes commencing electromagnetic stimulation. Instances of this occurrence are occasionally named induction boiler or Joule heating. In this report, we aim to scrutinize the influence of Ohmic heating on the radiative and dissipative flow of the micropolar flow of hybrid nanofluid within an inclined channel of length $2h$ under convective boundary conditions. Primary equations of the flow are renewed as the system of ODEs with the aid of proper similarity transmutations. The blend of shooting and Runge–Kutta 4th order approaches are utilized to get the desired outcomes on two occasions, i.e., hybrid fluid flow and micropolar fluid flow. The major findings of the current study are reported below:

- A larger pressure gradient minimizes fluid velocity.
- A larger inertia parameter minimizes the rotation profile in the case of micropolar fluid flow but ameliorates the same in the case of hybrid nanofluid flow.
- Escalation in Brinkmann number causes the amelioration in the fluid temperature.
- Magnetic field and radiation parameters mitigate the fluid temperature.
- Bi_2,Br,a_j, Ra and Gr are escalating the entropy generation.
- Gr Ameliorates the Bejan number near the midpoint of the channel and minimizes the same at other areas.

ζ	Makinde and Eegunjobi[42]	Present solutions
0	0	0
0.4	0.1138	0.1138
0.6	0.1215	0.1215
0.8	0.0868	0.0868
1	0	0

Table 2. Validation of the current solutions with existing literature when $\phi_1 = \phi_2 = Gr = M = Q_t = n$ $Ra = R = 0, A = \mathrm{Re} = 1, aj = 0$.

Data availability

The generated data during the current study available from the corresponding author on reasonable request.

Received: 17 January 2023; Accepted: 20 March 2023
Published online: 01 April 2023

References

1. Makinde, O. D. & Gbolagade, A. W. Second law analysis of incompressible viscous flow through an inclined channel with isothermal walls. *Rom. J. Phys.* **50**(9/10), 923 (2005).
2. Guimaraes, P. M. & Menon, G. J. Combined free and forced convection in an inclined channel with discrete heat source. *Int. Commun. Heat Mass Transf.* **35**, 1267–1274 (2008).
3. Dar, A. A. & Elangovan, K. Influence of an inclined magnetic field on Heat and mass transfer of the peristaltic flow of a couple stress fluid in an inclined channel. *World J. Eng.* **14**(1), 7–18 (2017).
4. Shahri, M. F. & Sarhaddi, F. Second law analysis for two-immiscible fluids inside an inclined channel in the presence of a uniform magnetic field and different types of nanoparticles. *J. Mech.* **34**(4), 541–549 (2018).
5. Javed, T., Hamid, A. H., Ahmed, B. & Ali, N. Effect of high Reynolds number on hydromagnetic peristaltic flow in an inclined channel using finite element method. *J. Korean Phys. Soc.* **71**(12), 950–962 (2017).
6. Hayat, T., Aslam, N., Khan, M. I., Khan, M. I. & Alsaedi, A. Physical significance of heat generation/absorption and Soret effects on peristalsis flow of pseudoplastic fluid in an inclined channel. *J. Mol. Liq.* **275**, 599–615 (2019).
7. Tlau, L. & Ontela, S. Second law analysis for mixed convection nanofluid flow in an inclined channel with convectively heated walls. *Heat Transf.* **49**(2), 1035–1064 (2020).
8. Adesanya, S. O., Souayeh, B., Rahimi-Gorji, M., Khan, M. N. & Adeyemi, O. G. Heat irreversibiility analysis for a couple stress fluid flow in an inclined channel with isothermal boundaries. *J. Taiwan Inst. Chem. Eng.* **101**, 251–258 (2019).
9. Singh, K., Pandey, A. K. & Kumar, M. Entropy generation impact on flow of micropolar fluid via an inclined channel with non-uniform heat source and variable fluid properties. *Int. J. Appl. Comput. Math.* **6**, 1–12 (2020).
10. Sabu, A. S., Mathew, A., Neethu, T. S. & George, K. A. Statistical analysis of MHD convective ferro-nanofluid flow through an inclined channel with hall current, heat source and soret effect. *Therm. Sci. Eng. Prog.* **22**, 100816 (2021).
11. You, X. & Li, S. Fully developed opposing mixed convection flow in the inclined channel filled with a hybrid nanofluid. *Nanomaterials* **11**(5), 1107 (2021).
12. Mathur, P., Mishra, S. R., Purohit, S. D. & Bohra, M. Entropy generation in a micropolar fluid past an inclined channel with velocity slip and heat flux conditions: Variation parameter method. *Heat Transf.* **50**, 7425–7439 (2021).
13. Prasad, K. V. *et al.* Slip flow of MHD Casson fluid in an inclined channel with variable transport properties. *Commun. Theor. Phys.* **72**(9), 095004 (2020).
14. Dutta, S., Bhattacharyya, S. & Pop, I. Two-phase model for mixed convection and flow enhancement of a nanofluid in an inclined channel patterned with heated slip stripes. *Int. J. Numer. Methods Heat Fluid Flow* (2021).
15. Gholinia, M., Gholinia, S., Hosseinzadeh, K. & Ganji, D. D. Investigation on ethylene glycol nano fluid flow over a vertical permeable circular cylinder under effect of magnetic field. *Results Phys.* **9**, 1525–1533 (2018).
16. Nadeem, S., Ahmed, Z. & Saleem, S. Carbon nanotubes effects in magneto nanofluid flow over a curved stretching surface with variable viscosity. *Microsyst. Technol.* **25**(7), 2881–2888 (2019).
17. Sowmya, G., Gireesha, B. J., Sindhu, S. & Prasannakumara, B. C. Investigation of Ti6Al4V and AA7075 alloy embedded nanofluid flow over longitudinal porous fin in the presence of internal heat generation and convective condition. *Commun. Theor. Phys.* **72**(2), 025004 (2020).
18. Dogonchi, A. S., Chamkha, A. J., Hashemi-Tilehnoee, M., Seyyedi, S. M. & Ganji, D. D. Effects of homogeneous-heterogeneous reactions and thermal radiation on magneto-hydrodynamic Cu–water nanofluid flow over an expanding flat plate with non-uniform heat source. *J. Central South Univ.* **26**(5), 1161–1171 (2019).
19. Anuar, N. S., Bachok, N., Arifin, N. M. & Rosali, H. Analysis of Al_2O_3-Cu nanofluid flow behaviour over a permeable moving wedge with convective surface boundary conditions. *J. King Saud Univ. Sci.* **33**(3), 101370 (2021).
20. Waqas, H., Farooq, U., Alghamdi, M. & Muhammad, T. Significance of surface-catalyzed reactions in SiO_2-H_2O nanofluid flow through porous media. *Case Stud. Therm. Eng.* **27**, 101228 (2021).
21. Jamshed, W. & Aziz, A. Cattaneo-Christov based study of Casson hybrid nanofluid flow over a stretching surface with entropy generation. *Appl. Nanosci.* **8**(4), 685–698 (2018).
22. Salman, S., Talib, A. A., Saadon, S. & Sultan, M. H. Hybrid nanofluid flow and heat transfer over backward and forward steps: A review. *Powder Technol.* **363**, 448–472 (2020).
23. Abbas, N., Malik, M. Y., Nadeem, S. & Alarifi, I. M. On extended version of Yamada-Ota and Xue models of hybrid nanofluid on moving needle. *Eur. Phys. J. Plus* **135**(2), 1–16 (2020).
24. Anuar, N. S., Bachok, N. & Pop, I. (2020). Radiative hybrid nanofluid flow past a rotating permeable stretching/shrinking sheet. *Int. J. Numer. Methods Heat Fluid Flow*.
25. Waini, I., Ishak, A. & Pop, I. Hybrid nanofluid flow over a permeable non-isothermal shrinking surface. *Mathematics* **9**(5), 538 (2021).
26. Ahmad, F. *et al.* The improved thermal efficiency of Maxwell hybrid nanofluid comprising of graphene oxide plus silver/kerosene oil over stretching sheet. *Case Stud. Therm. Eng.* **27**, 101257 (2021).
27. Rashid, U. *et al.* Study of (Ag and TiO2)/water nanoparticles shape effect on heat transfer and hybrid nanofluid flow toward stretching shrinking horizontal cylinder. *Results Phys.* **21**, 103812 (2021).
28. Khan, U., Waini, I., Ishak, A. & Pop, I. Unsteady hybrid nanofluid flow over a radially permeable shrinking/stretching surface. *J. Mol. Liq.* **331**, 115752 (2021).
29. Salahuddin, T., Bashir, A. M., Khan, M., & Chu, Y. M. A comparative analysis of nanofluid and hybrid nanofluid flow through endoscope. *Arab. J. Sci. Eng.* 1–10 (2021).
30. Rasool, G., Wakif, A., Wang, X., Shafiq, A. & Chamkha, A. J. Numerical passive control of alumina nanoparticles in purely aquatic medium featuring EMHD driven non-Darcian nanofluid flow over convective Riga surface. *Alex. Eng. J.* **68**, 747–762 (2022).
31. Shah, N. A. *et al.* Significance of nanoparticle's radius, heat flux due to concentration gradient, and mass flux due to temperature gradient: The case of water conveying copper nanoparticles. *Sci. Rep.* **11**(1), 1882 (2021).
32. Rasool, G. *et al.* Hydrothermal and mass aspects of MHD non-Darcian convective flows of radiating thixotropic nanofluids nearby a horizontal stretchable surface: Passive control strategy. *Case Stud. Therm. Eng.* **42**, 102654 (2023).
33. Raju, C. S. K. *et al.* Non-linear movements of axisymmetric ternary hybrid nanofluids in a thermally radiated expanding or contracting permeable Darcy walls with different shapes and densities: Simple linear regression. *Int. Commun. Heat Mass Transf.* **135**, 106110 (2022).
34. Maneengam, A. *et al.* Entropy generation in 2D lid-driven porous container with the presence of obstacles of different shapes and under the influences of Buoyancy and Lorentz Forces. *Nanomaterials* **12**(13), 2206 (2022).

35. Raju, C. S. K., and Se-Jin Yook. "Exact solution of Non-linear free convective with longitudinal slits in the presence of super hydrophobic and non-hydrophobic microchannels filled by nanoparticles: Multi-Linear Regression Analysis." Korean Society of Mechnaical Engineers, Spring and Autumn Conference, (2022) 985–985.
36. Rasool, G., Shah, NA., El-Zahar, ER. & Wakif, A. Numerical investigation of EMHD nanofluid flows over a convectively heated riga pattern positioned horizontally in a Darcy-Forchheimer porous medium: Application of passive control strategy and generalized transfer laws. Waves Random Complex Media 1–20 (2022).
37. Reddy, S. R. R., C. S. K. Raju, Sreedhara Rao Gunakala, H. Thameem Basha, and Se-Jin Yook. "Bio-magnetic pulsatile CuO– Fe3O4 hybrid nanofluid flow in a vertical irregular channel in a suspension of body acceleration." International Communications in Heat and Mass Transfer 135 (2022): 106151.
38. Srinivasacharya, D. & Himabindu, K. Effect of slip and convective boundary conditions on entropy generation in a porous channel due to micropolar fluid flow. *Int. J. Non-linear Sci. Numer. Simul.*, 2016-0056.
39. You, X. & Li, S. Fully developed opposing mixed convection flow in the inclined channel filled with a hybrid nanofluid. *Nanomaterials (Basel)* **11**(5), 1107 (2021).
40. Roja, A., Gireesha, B. J. & Nagaraja, B. Irreversibility investigation of Casson fluid flow in an inclined channel subject to a Darcy-Forchheimer porous medium: A numerical study. *Appl. Math. Mech.* **42**(1), 95–108 (2021).
41. Al-Hossainy, A. F. & Eid, M. R. Combined experimental thin films, TDDFT-DFT theoretical method, and spin effect on [PEG-H_2O/ZrO2+ MgO] h hybrid nanofluid flow with higher chemical rate. *Surf. Interfaces* **23**, 100971 (2021).
42. Makinde, O. D. & Eegunjobi, A. S. Effects of convective heating on entropy generation rate in a channel with permeable walls. *Entropy* **15**(1), 220–233 (2013).

Author contributions

S.S.K.R.: Conceptualization, Investigation, Writing—original draft, Writing—review & editing, Methodology, Formal analysis, Resources, Writing—original draft, Writing—review & editing. Validation, Data curation, Software.

Funding

This work was supported by the Deanship of Scientific Research, Vice Presidency for Graduate Studies and Scientific Research, King Faisal University, Saudi Arabia [Grant No. 893].

Competing interests

The author declares no competing interests.

Additional information

Correspondence and requests for materials should be addressed to S.S.K.R.

Reprints and permissions information is available at www.nature.com/reprints.

Publisher's note Springer Nature remains neutral with regard to jurisdictional claims in published maps and institutional affiliations.